GUIDANCE TRADES FOR HIGH BALLISTIC COEFFICIENT MARS LANDER TRAJECTORIES

Tyler R. Anderson*
Georgia Institute of Technology, Atlanta, Georgia **Robert D. Braun**†
University of Colorado Boulder, Boulder, CO

Large ballistic coefficient entry vehicles are required to achieve more ambitious exploration goals at Mars. These trajectories exhibit several characteristics that make successful landings difficult including low altitude deceleration and inability to decelerate under parachute. One promising mission architecture involving propulsive supersonic descent and landing is proposed as a candidate for future high ballistic-coefficient vehicles. This paper will investigate guidance options for precision landing using hypersonic bank-angle steering and thrust vector controlled propulsive descent. First, a numerical predictor-corrector guidance algorithm is applied to examine the benefits and trade-offs of range targeting during the hypersonic regime. This is compared against the state-of-the-art Apollo Final Phase guidance algorithm. Next, a modification is included to increase guidance performance. Finally, a propulsive divert algorithm is assessed for its impact on landing accuracy and propellant usage.

NOMENCLATURE

CDF = Cumulative Distribution Function

EDL = Entry, Descent, and Landing

$FNPEG$ = Fully Numerical Predictor-Corrector Entry Guidance

$G\text{-}FOLD$ = Guidance for Fuel-Optimal Large Divert

h_0 = Initial altitude

I_{sp} = Specific Impulse

JPL = Jet Propulsion Laboratory

L/D = Lift-to-Drag ratio

MSL = Mars Science Laboratory

$MOLA$ = Mars Orbiter Laser Altimeter

T/W = Total vehicle thrust-to-weight ratio

*Graduate Research Assistant, School of Aerospace Engineering, 270 Ferst Dr., Member AIAA.
†Dean of the College of Engineering and Applied Science and Professor of Aerospace Engineering Sciences

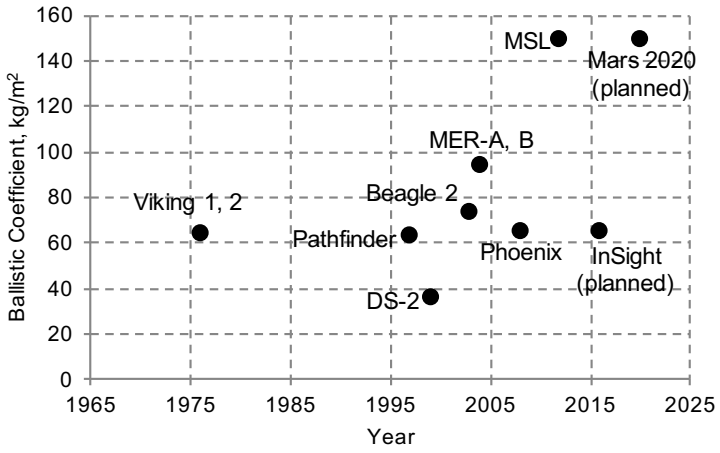

Figure 1. Ballistic coefficients of previous Mars landers.[1]

TDI = Terminal Descent Initiation

V_0 = Initial planet-centered inertial velocity

β = Ballistic coefficient

γ = Initial inertial flight path angle

λ = FNPEG energy blending variable

INTRODUCTION

MANNED Mars missions will require a paradigm shift in how we accomplish Entry, Descent, and Landing. These missions will necessarily include multiple high-mass payloads landing within walking distance of each other. At the same time, launch vehicle capabilities place constraints on the maximum diameter of aeroshells, which means high ballistic-coefficient vehicles will be required. Achieving sufficient deceleration while retaining adequate timeline and altitude to execute terminal descent remains one of the primary challenges of landing vehicles on Mars. Additionally, precision landing is required to enable access to a wider variety of scientifically interesting sites and to position assets for human landings.[1]

Early Mars lander missions maintained relatively small ballistic coefficients near 60 kg/m^2 to enable greater deceleration in the hypersonic regime (see Fig. 1). More recently, the Mars Science Laboratory (MSL) has pushed the upper bound of what is possible with a 145 kg/m^2 ballistic coefficient. Landing a 1 t payload, MSL represents the state-of-the-art. New supersonic descent options will be required to increase landed payload masses. Multiple technology options are being explored to mitigate this issue: lightweight deployable drag devices to reduce the ballistic coefficient for higher-mass vehicles,[2] high-performance parachutes to improve terminal descent margins,[3] and supersonic retropropulsion to increase deceleration during descent.[4] [5] Of these, supersonic retropropulsion is the easiest to scale to larger payloads and may be the only option for the large payload masses associated with human-class missions.[6]

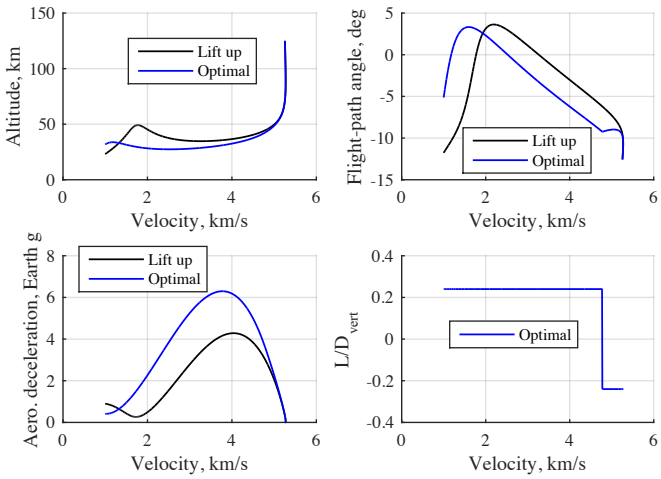

Figure 2. Example trajectory a) altitude, b) flight-path angle, c) deceleration, and d) vertical L/D as functions of relative velocity.

High ballistic coefficient vehicles tend to decelerate low in the atmosphere, which decreases descent timelines and restricts landing locations to low-lying areas. Previous work has examined trajectory options for increasing terminal descent altitudes. [7] It is proposed that this method is also an effective way to decrease the required propellant mass fraction for a given vehicle mass using supersonic propulsive descent and landing. However, this work did not consider guidance options and range targeting to improve robustness in dispersed environments. As Garcia-Llama and others have shown, optimal trajectories often are not robust to atmospheric and vehicle uncertainties in-flight[8]. This paper will examine the effect of a numerical predictor-corrector range targeting algorithm applied to trajectories with a bank reversal. These techniques may be applicable to future large-scale robotic or human EDL architectures [5]. In addition, the performance trades-offs of propulsive descent guidance will be overviewed.

Benefits of Bang-Bang Trajectory

Previous work by Anderson, et al. demonstrated the altitude raising effects of a bank angle reversal during hypersonic flight. [7] Fig. 2 demonstrates this effect with two trajectories for an MSL-like vehicle: a full-lift-up trajectory with $u = L/D_{max}$ (the Viking strategy) and an altitude optimal bang-bang trajectory, where u changes sign near 5 km/s (Fig. 2d). The trajectory terminates at an arbitrarily chosen velocity. To assess a more realistic terminal condition, this trajectory is re-formulated as follows: a simple propulsive descent controller is included to land the vehicle at a pre-specified altitude. A propellant mass fraction is calculated, and the bank-reversal point is be chosen to minimize the propellant mass used. For this purpose, a reference case is chosen and outlined in Table 1.

The optimization problem is a simple single-parameter search for the bank reversal time. A soft constraint keeps the minimum altitude at least 600 m above the target altitude, since optimal trajectories tend to fly low before lofting. This optimal trajectory is shown with a fully lift-up trajectory in Fig. 3. The optimal trajectory uses 19.0 percent of the entry mass for fuel, while the lift-up trajectory uses 29.8 percent. While this comes at a cost of increasing the peak G-loading

Table 1. Reference Trajectory Parameters

Parameter	Value
β	450 kg/m^2
L/D	0.24
h_0	125 km
V_0	6.5 km/s
γ_0	-16°
Engine I_{sp}	300 s
T/W	3
Target alt	-500 km MOLA

from 11 to 15 g's, it is clear that an initial bank-down trajectory could significantly increase the payload capacity of a high-ballistic coefficient Mars vehicle.

Hypersonic Guidance

Previous Mars vehicles have usually flown an unguided lift-up trajectory or ballistic entry. The Mars Science Laboratory was the first mission to include a form of bank-steering for range targeting.[9] The algorithm used was a modified form of the Apollo Final-Phase,[10] which takes a nominal trajectory and computes gains using backwards integration of the adjoint equations of motion. It then computes the bank angle using these gains based on the measured altitude rate and drag force. This algorithm is remarkably accurate in well-known environments when the vehicle is able to closely follow the reference trajectory. However, deviations from this reference tend to cause growing errors in range targeting. More modern algorithms have been developed that are able to harness the massively increased computing power available since the Apollo program. One of these is called the Fully Numerical Predictor-Corrector Entry Guidance algorithm (FNPEG).[11] Numerical predictor-corrector algorithms propagate the expected trajectory numerically and correct the bank angle to minimize the predicted downrange error. This algorithm has been tested for low-lifting vehicles on Earth, but it has not been examined in the context of bang-bang trajectories for Mars entry.

Propulsive Guidance

The gravity turn, a maneuver in which the thrust vector is aligned with the velocity vector, has been the simplest guidance option for decades. A gravity turn controller was used to land the lunar lander during the Apollo missions. The benefit of the gravity turn is it's simplicity of implementation and the fact that the final flight-path angle is -90 degrees. However, it is not a fuel-optimal maneuver. Joel Benito at JPL calculated that the minimum fuel solution from a given state to rest at the target altitude is actually a constant thrust angle.[12] That is, the vehicle finds the constant angle with respect to the ground that results in zero velocity. It then calculates the altitude loss during this burn, and initiates the burn if the predicted landing altitude is at the target. A trajectory produced by this optimal propulsive guidance is compared against the gravity turn in Fig. 4.

Since propellant usage is directly related to burn time, an algorithm that can delay the TDI point will save on fuel costs. The optimal solution does this by causing the vehicle to follow a straight line to the final target in the velocity space, seen in the bottom righthand corner of Fig. 4. The propellant mass fractions for this trajectory are 22.9% and 20.2% for the gravity turn and optimal guidance, respectively. The optimal guidance was used for all of the studies in this paper.

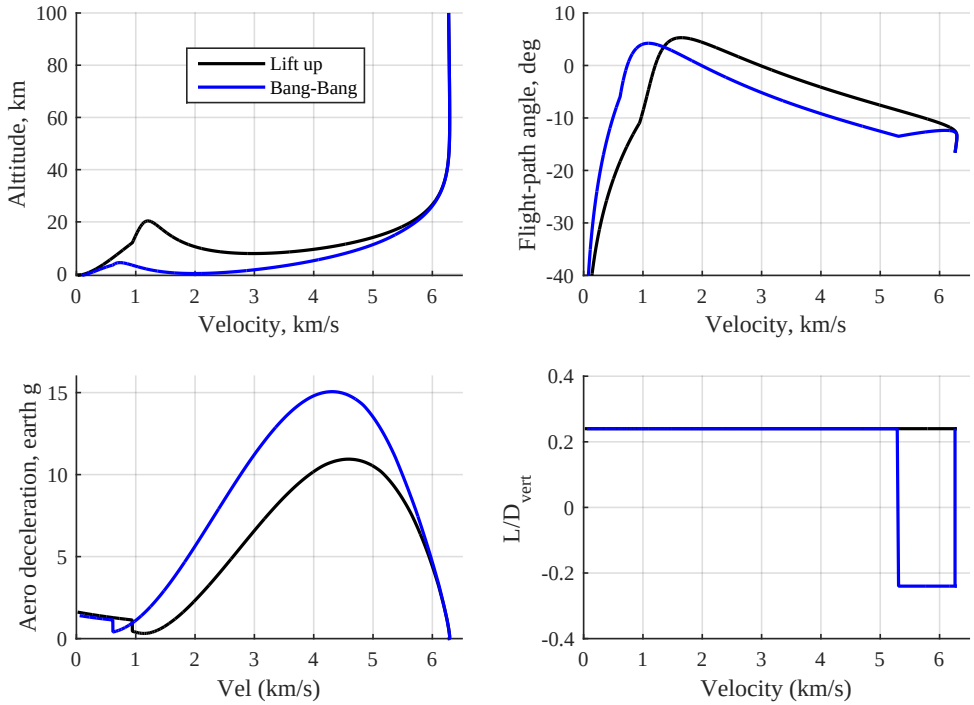

Figure 3. Comparison of full lift-up and bang-bang trajectories

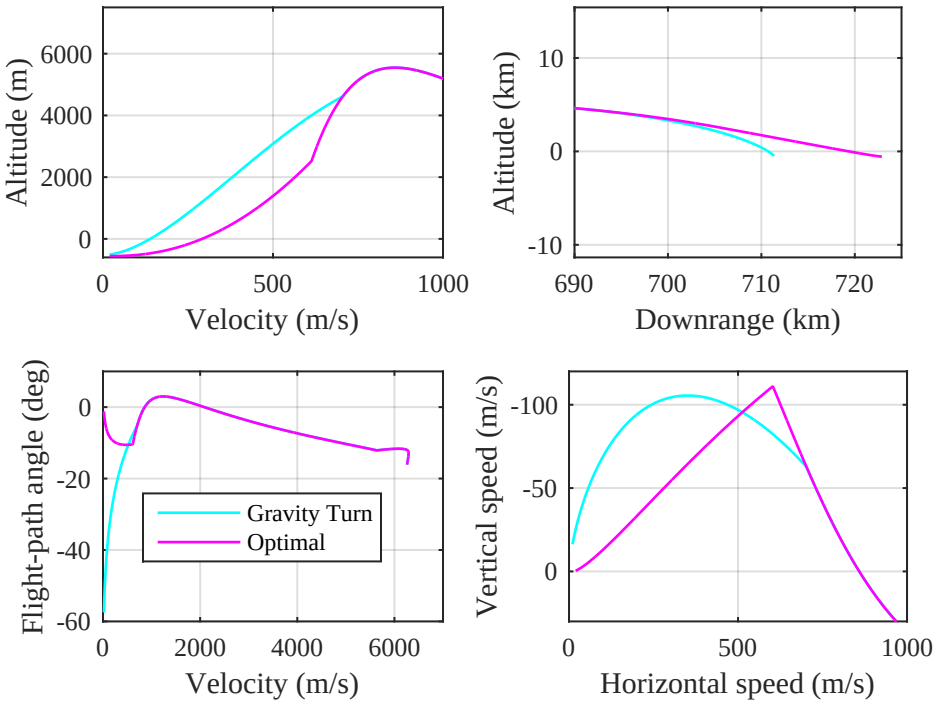

Figure 4. Propulsive Descent Guidance Comparison

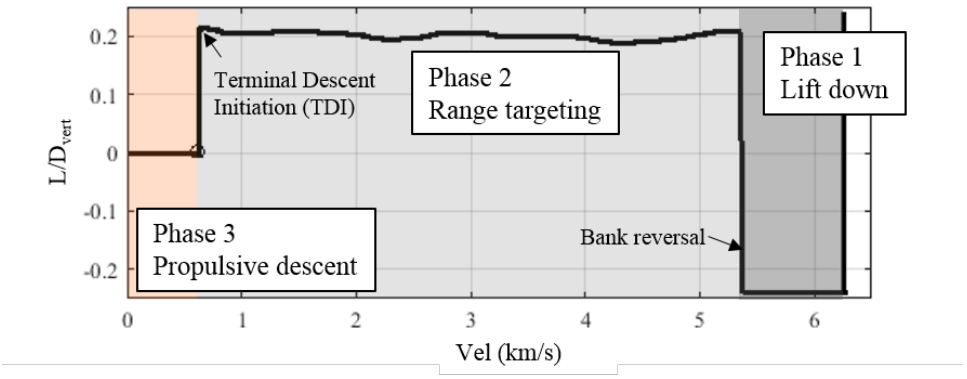

Figure 5. Nominal Trajectory Control

The optimal propulsive guidance provides a baseline for fuel consumption, but in practice a targeting guidance algorithm will be required for precision propulsive landing. One promising algorithm is Guidance for Fuel-Optimal Large Divert (G-FOLD),[13] developed at JPL. This algorithm uses convex optimization to compute the minimum fuel trajectory to a specified landing site while respecting control and trajectory constraints.

ANALYSIS AND RESULTS

All trajectory simulations used in this paper were performed using ASIM, a 3 degree-of-freedom flight mechanics simulation developed at Georgia Tech. Vehicle motion is assumed to be planar, though a higher fidelity analysis would have some error contribution from cross-range control and heading alignment. The assumed reference trajectory is as follows: in phase 1, the vehicle enters the atmosphere lift-down (at a bank angle of 180 degrees) until some point chosen to minimize fuel usage during terminal descent. It then switches to a constant bank angle in phase 2. In phase 3 the vehicle uses the optimal propulsive descent to land at the target altitude. This is shown schematically as a function of vertical L/D in Fig. 5.

Based on this reference trajectory, the nominal states at the bank reversal point and at TDI can be found. These are used as targets for the switch from phase 1 to phase 2 and phase 2 to 3, respectively. In flight, the vehicle flies fully lift down in phase 1 until it hits some trigger defined by the reference trajectory. In phase 2 it performs bank-angle modulation (with FNPEG or Apollo) to target the TDI range from the nominal trajectory. The propulsive descent is initiated based on the optimal propulsive guidance described in Section . The Monte-Carlo analyses performed use 1000 runs with the Gaussian distributed dispersions listed in 2. Since these algorithms are nominally used to target the downrange at terminal descent initiation, a good measure of performance is the distribution of range errors. Propellant mass fraction usage is also a key performance indicator. Secondary performance indicators include how close the trajectories come to the nominal TDI velocity, altitude, and flight-path angle.

Phase 1

The benefits of the bang-bang trajectory come from control authority granted by the high dynamic pressure generated during the bank-down flight in phase 1. While range targeting and other

Table 2. Reference Trajectory Parameters

Parameter	3-σ dispersion
Entry mass	2 kg
C_l	0.04
C_d	0.02
V_0 magnitude	2 m/s
γ_0	0.2 deg
R_0	200 m
density	20%

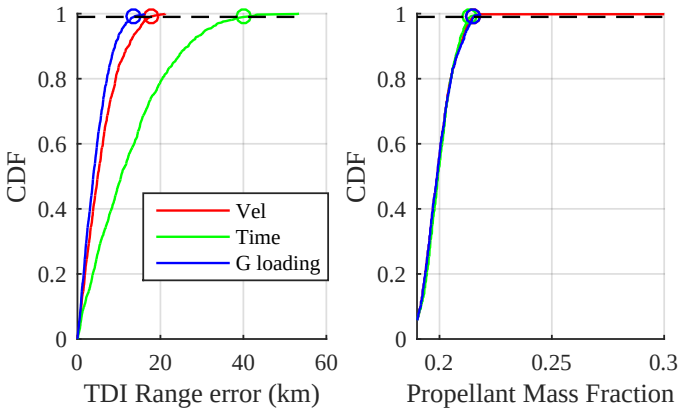

Figure 6. Bank Reversal Trigger Range Performance

maneuvers could occur during this portion, for this paper it is assumed that the vehicle stays fully lift-down during the entire phase in order to achieve the maximum benefit. Therefore, the primary guidance question in phase 1 is how to determine when to initiate the bank reversal and switch to phase 2. This topic was covered briefly by Anderson et al,[7] but only at a very high level and led to elementary insights. The use of velocity, time, and g-loading bank reversal triggers and bank-angle steering is investigated to determine their effect on terminal descent initiation. The triggers are implemented as follows: the nominal trajectory is found by the same mass fraction optimization described above. The state at bank reversal (time, velocity, and g-loading) is picked out and used as a trigger state. During flight, the vehicle state is monitored and the bank reversal is initiated when the trigger condition is met. Since time and velocity are nearly always monotonic along the trajectory, most trajectories are guaranteed to reach the trigger condition at some point. G-loading, however, reaches a maximum at some point after the trigger condition. If the trigger loading is close to the maximum loading along the nominal trajectory, there is a chance that a vehicle flying through slightly different conditions will never reach the trigger condition. In this case, the bank reversal is set to occur once the G-loading hits tits maximum. Thus, having three different conditions for initiating the bank reversal, the robustness of the bank reversal triggers can be assessed. The Apollo algorithm is used for range guidance during the portion of the trajectory after bank reversal. Results are shown in Figs. 6 and 7.

The three bank reversal trigger produce similar results in TDI state. That is, the Apollo algorithm

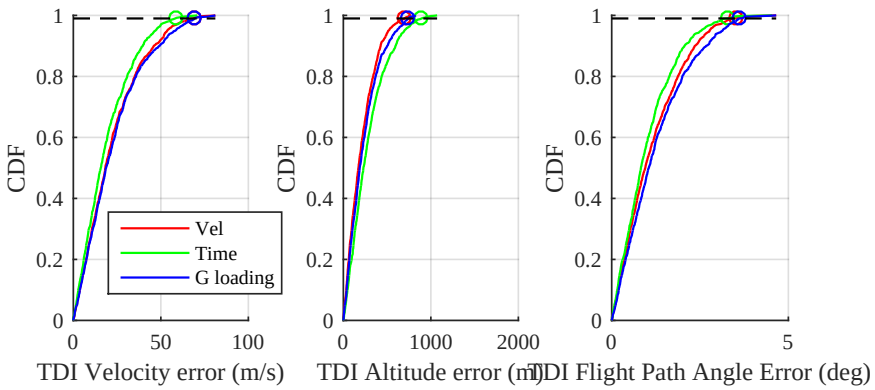

Figure 7. Bank Reversal Trigger TDI State Performance

effectively reaches the nominal TDI state regardless of the trigger used to initiate the bank reversal. However, the range errors vary with the G-loading trigger producing the smallest range errors (13 km at the 99% level) and the time trigger producing the greatest (40 km at the 99% level). The G-loading trigger was used for the remaining results in this paper.
Note that the above was only a first look at possible triggering mechanisms that could be implemented in a flight vehicle. It is possible to use state feedback and adjust the trigger point in-flight in order to improve range and/or propellant performance. This is left to future work.

Phase 2

The algorithm used for range targeting during Phase 2 has the greatest effect on trajectory accuracy. To assess how they behave nominally, the FNPEG and Apollo trajectories are shown with no dispersions in Fig. 8. While some error is to be expected, the two guidance methods are able to command close to the nominal bank angle and reach the target state with minimal error. The state at propulsive descent initiation is shown as circles in the appropriate colors.

Focus is now turned to the performance of these algorithms in dispersed cases. An open-loop control with the bank angle magnitude fixed at a constant $30\,\mathrm{deg}$ is shown for comparison in Fig. 9.

Clearly, in the current configuration the Apollo algorithm performs better than FNPEG, with a 99% range error at terminal descent initiation (TDI) of 7 and 35% km respectively. The reason for this large error in FNPEG seems be the propagation of small errors introduced with the simplifications of the equations of motion, such as a non-rotating planet and constant gravity. A way to correct for this is presented in the following section. The altitude, velocity, and flight-path angle errors are compared along with the total propellant mass fraction in Fig. 10. Here the differences between the two algorithms are less stark, although the Apollo algorithm is able to reach the nominal TDI velocity better than FNPEG.

FNPEG Energy Formulation FNPEG works by choosing an energy-like variable $e = \frac{1}{r} - \frac{V^2}{2}$ as the domain of integration in the predictor function. This variable was chosen because it is monotonic along and because the initial and final energy can be fully defined in terms of the initial and target states. However, any similar variable that retains these properties would be an equally acceptable

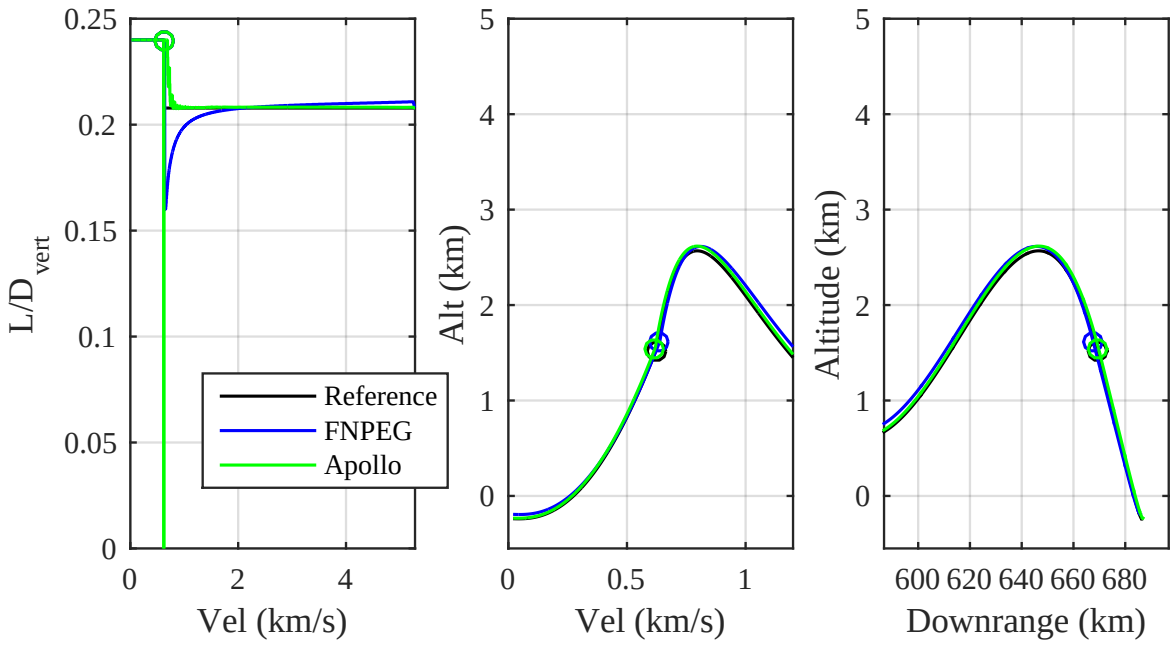

Figure 8. Nominal guidance performance

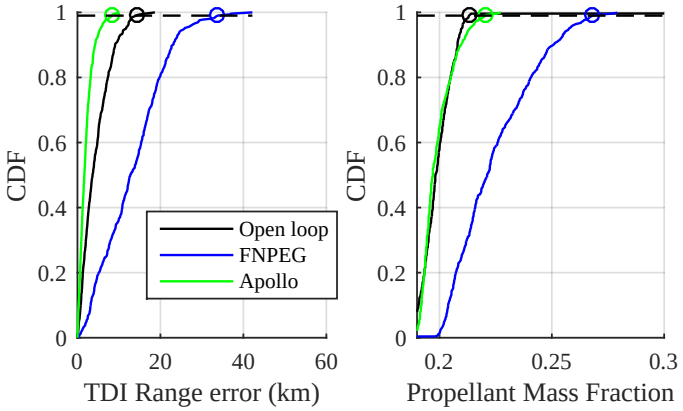

Figure 9. Dispersed Guidance Range and PMF Performance

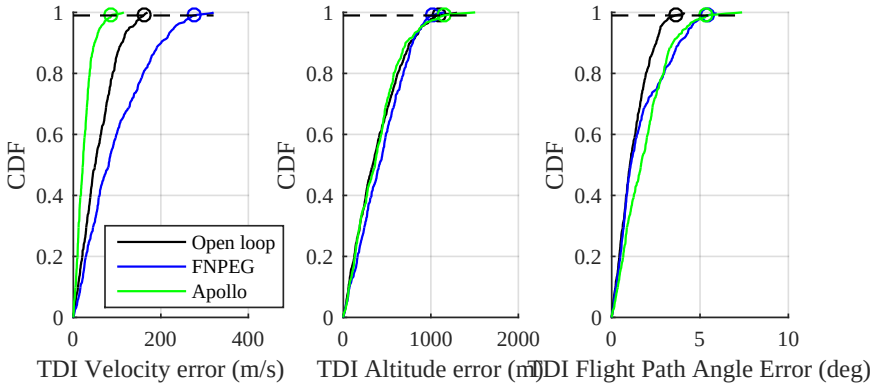

Figure 10. Dispersed Guidance TDI State Performance

domain. Let us redefine the energy domain variable according to Eq. 1 where λ is a blending variable that alters the relative contribution of velocity and position to the energy. The corresponding derivative $\frac{de}{d\tau}$ is given in Eq. 2

$$e = (1-\lambda)\frac{2}{r} - \lambda V^2 \tag{1}$$

$$\frac{de}{d\tau} = \frac{2V\sin\gamma}{r^2}(2\lambda - 1) + 2\lambda DV \tag{2}$$

Notice that a value of $\lambda = 0.5$ makes the energy variable equivalent to the initial formulation. Since it is still a function of position and velocity, this variable is still defined as a function of the vehicle state. Note for any $\lambda > 0.5$ there is the possibility that $\frac{de}{d\tau} < 0$ at the beginning of the trajectory when $\gamma < 0$ and drag D is very small. To show that e is monotonically increasing in the region of validity regardless of the value of λ, several curves were plotted along the nominal trajectory defined in Table 1. This is shown in Fig. 11.

The energy is increasing at all points after bank reversal, indicated by the dotted line. Therefore, this new blended energy variable would be a good candidate for a domain of integration.
We want to find the optimum value of λ to maximize the performance of the FNPEG algorithm. This may make a difference in the propellant mass fraction used, since the terminal descent initiation point is a function of both position and velocity. By changing the target energy formulation, the algorithm can more accurately achieve the target velocity or position depending on the needs of the problem. State dispersion CDF's for different λ are shown in Figs. 12 and 13.

Interestingly, it appears that the best performance comes from very low values of λ. A value of $\lambda = 0.045$ gives the smallest propellant mass fraction usage and the smallest range error at the 99% level. In fact the only reason λ was not decreased further was because it led to numerical issues in certain cases (since velocity still has to be calculated from e in the predictor algorithm). These results suggest that alternative formulations of the domain of integration can alter the performance of numerical predictor-corrector algorithms. This blended energy term is by no means the only candidate. The angular momentum magnitude, which is also defined by velocity and position and is a monotonically decreasing function of time, could also be used.
A remark on the use of predictor-correctors for entry guidance: the power of FNPEG comes from

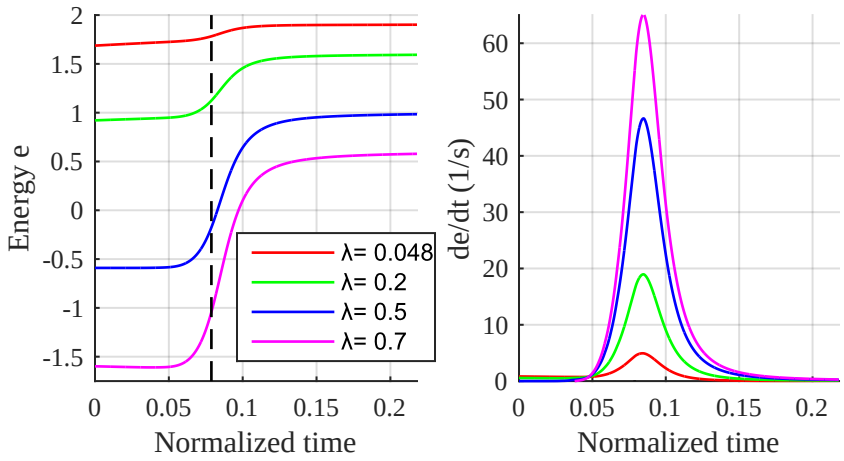

Figure 11. Energy and Energy Derivative in Nominal Trajectory

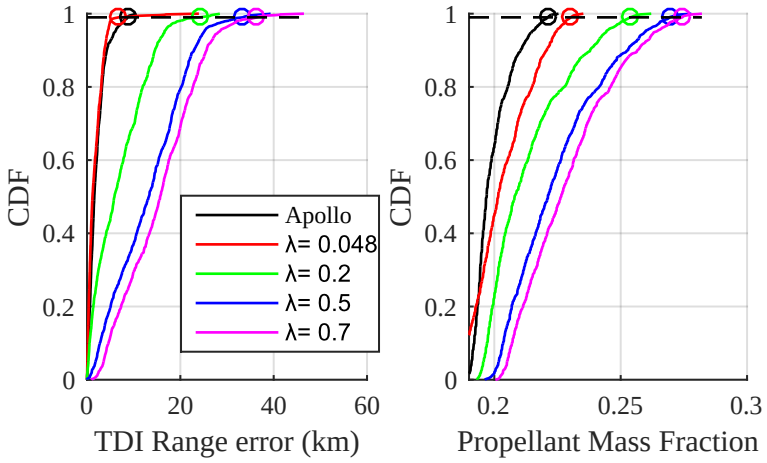

Figure 12. Range and PMF performance for various λ

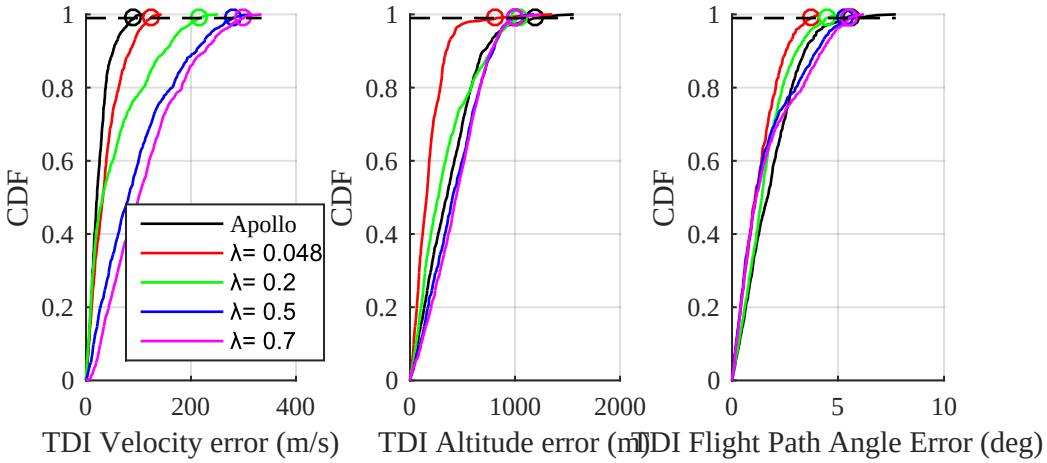

Figure 13. TDI State performance for various λ

the simplicity of the underlying problem formulation. The introduction of a blending term is one of many simple improvements that can be made.[14] For instance, having a direct model of the atmosphere in the predictor loop could allow for real-time updating of the atmospheric density estimate. This does not rely on the introduction of gains and linear approximations that many optimal control algorithms (such as LQR trajectory tracking) require. For future high-ballistic coefficient missions where the margins for success may be small, algorithms like FNPEG could play a key role.

Phase 3

We turn our attention finally to the issue of propulsive divert. While hypersonic guidance is effective at delivering vehicles close to the target point, the propulsive descent guidance is ultimately responsible for taking out any remaining position error. For this purpose, G-FOLD is a good candidate fuel-optimal algorithm. G-FOLD is assessed by first performing a 1000-run Monte-Carlo analysis with Apollo hypersonic guidance. The state of the vehicle (velocity, position, and flight-path angle) at the ignition point is used as an input to G-FOLD. The target condition is the final point of the nominal trajectory using the optimal propulsive guidance. Note that G-FOLD will allow for a period of free-fall prior to thrusting if it will lower propellant usage, so these starting conditions would not necessarily optimal if G-FOLD were fully integrated into the guidance. Results are shown in Fig. 14.

G-FOLD is able to null all range errors and still use slightly less propellant than the gravity turn. Relative to the optimal descent guidance, G-FOLD is able to null up to 5 km of range error at a cost of about 4.3% additional propellant mass. Note also that the pmf cost of using G-FOLD falls between that of the optimal propulsive guidance and gravity turn. Based on this limited case study, these two simple descent algorithms may offer a bounding guess of the cost of precision propulsive landing.

CONCLUSIONS

Various guidance options for high-ballistic coefficient Mars entry vehicles were studied. A nominal trajectory was found which is broken into three phases: first, the vehicle flies lift-down until

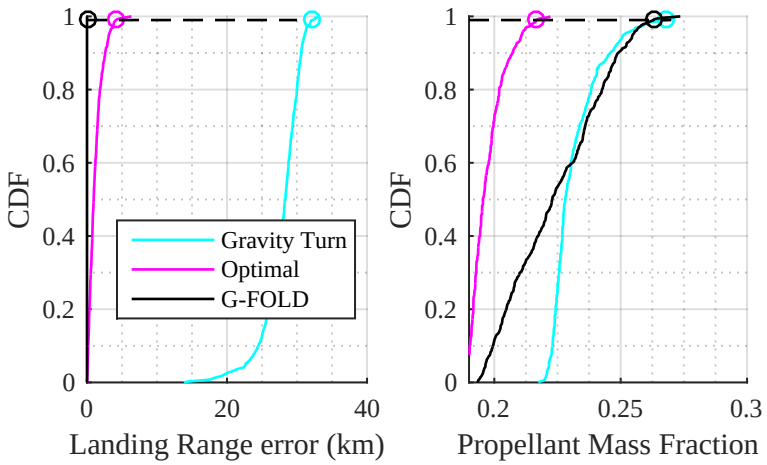

Figure 14. G-FOLD Performance Benefits

some point chosen to maximize total propellant mass usage. Second, the vehicle flies nearly lift-up and modulates the bank angle in order to hit a downrange target. Finally, propulsive descent guidance brings the vehicle to rest at the target altitude. This trajectory can reduce propellant mass fractions for heavy entry vehicles that employ supersonic retropropulsion. Guidance options were assessed for controlling this trajectory. In particular, the legacy Apollo Final Phase algorithm was compared against a newer predictor-corrector algorithm called FNPEG. An improvement was applied to this algorithm that allows engineers to tune performance for a particular problem. Guidance performance was assessed by looking at the distribution of downrange errors at terminal descent initiation, which is a proxy for landing site error. State errors at terminal descent as well as propellant mass usage were also presented as performance metrics. Finally, a cursory analysis of G-FOLD propulsive divert guidance was performed to gain some insight into the trade-off's of precision landing.

Next steps in this work include testing this trajectory and these guidance options across a range of entry vehicles and entry conditions. Further improvements can be made to both the FNPEG and Apollo algorithms to make them more applicable to the presented entry architecture. Introduction of G-FOLD directly into the simulation would provide a full end-to-end trajectory solution that could be implemented into a flight vehicle without substantial alteration.

REFERENCES

[1] Braun, R. D. and Manning, R. M., "Mars Exploration Entry, Descent, and Landing Challenges," *Journal of Spacecraft and Rockets*, Vol. 44(2), March–April 2007, pp. 310–323.

[2] Hughes, Stephen J., Cheatwood, Dr. F McNeil, Dillman, Robert A., Wright, Henry S., DelCorso, Joseph A., "Hypersonic Inflatable Aerodynamics Decelerator (HIAD) Technology Development Overview," AIAA 2011-2524, May 2011.

[3] Clark, I. G., Adler, M., and Rivollini, T., "Development and Testing of a New Family of Supersonic Decelerators," AIAA 2013-1252, Mar. 2013.

[4] Korzun, A. M., Braun, R. D., and Cruz, J. R., "Survey of Supersonic Retropropulsion Technology for Mars Entry, Descent, and Landing," *Journal of Spacecraft and Rockets*, Vol. 46(5), Sep. 2009, pp. 929–937.

[5] Price, H.P.; Braun, R.D.; Manning, R.M.; and Sklyanski, E.; "A High-Heritage Blunt-Body Entry, Descent, and Landing Concept for Human Mars Exploration," 2016 AIAA Science and Technology Forum and Exposition, San Diego, CA, January 2016.

[6] Edquist, K. T., et al. "Development of Supersonic Retropropulsion for a Mars Precursor Mission." LPI Contributions 1679 (2012): 4151.

[7] Anderson, T.R., Putnam, Z.R., and Braun, R.D., "Strategies for Landing Large Ballistic Coefficient Vehicles on Mars", *AIAA Atmospheric Flight Mechanics Conference*, AIAA SciTech, (AIAA 2016-0021)

[8] Garcia-Llama, E., "Apollo-Derived Terminal Control for Bank-Modulated Mars Entries with Altitude Maximization," AIAA 2008-6819, Aug. 2008.

[9] Mendeck, Gavin F., and Craig, Lynn E. "Entry Guidance for the 2011 Mars Science Laboratory Mission." AIAA Atmospheric Flight Mechanics Conference and Exhibit, Aug. 2011.

[10] Moseley, P. E., "The Apollo Entry Guidance: A Review of the Mathematical Development and Its Operational Characteristics", TRW Note No. 69-FMT-791, TRW, December 1, 1969

[11] Ping Lu. "Predictor-Corrector Entry Guidance for Low-Lifting Vehicles", *Journal of Guidance, Control, and Dynamics*, Vol. 31, No. 4 (2008), pp. 1067-1075.

[12] Benito, Joel; Brandeau, Erich; Skylanskiy, Evgeniy; and Sell, Steve; "Powered Descent Guidance Strategy and Algorithms for Mars Landing Using Supersonic Retropropulsion," 2017 IEEE Aerospace Conference, Big Sky, Montana

[13] B. Acikmese, J. Casoliva, J. M. Carson, and L. Blackmore. "G-FOLD: A Real-Time Implementable Fuel Optimal Large Divert Guidance Algorithm for Planetary Pinpoint Landing". In Concepts and Approaches for Mars Exploration, Vol. 1679 of LPI Contributions, page 4193, June 2012.

[14] Ping Lu. "Entry Guidance: a Unified Method", *Journal of Guidance, Control, and Dynamics*, Vol. 37, No. 3, pp. 713–728, 2014